Virology 484 (2015) 136–145

Contents lists available at ScienceDirect

Virology

journal homepage: www.elsevier.com/locate/yviro

Glycoprotein 5 of porcine reproductive and respiratory syndrome virus strain SD16 inhibits viral replication and causes G2/M cell cycle arrest, but does not induce cellular apoptosis in Marc-145 cells

Yang Mu [a,b], Liangliang Li [a,b], Beibei Zhang [a,b], Baicheng Huang [a,b], Jiming Gao [a,b], Xiangpeng Wang [a,b], Chengbao Wang [a,b], Shuqi Xiao [a,b], Qin Zhao [a,b], Yani Sun [a,b], Gaiping Zhang [a,c], Julian A. Hiscox [a,d], En-Min Zhou [a,b,*]

[a] Department of Preventive Veterinary Medicine, College of Veterinary Medicine, Northwest A&F University, No. 22 Xinong Road, Yangling, Shaanxi 712100, China
[b] Experimental Station of Veterinary Pharmacology and Veterinary Biotechnology, Ministry of Agriculture of the People's Republic of China, No. 22 Xinong Road, Yangling, Shaanxi 712100, China
[c] College of Animal Science and Veterinary Medicine, Henan Agricultural University, Zhengzhou, Henan 450002, China
[d] Department of Infection Biology, Institute of Infection and Global Health, University of Liverpool, Liverpool L3 5RF, UK

ARTICLE INFO

Article history:
Received 31 October 2014
Returned to author for revisions
23 March 2015
Accepted 30 May 2015
Available online 19 June 2015

Keywords:
PRRSV
GP5
Cell apoptosis
Virus replication
IFN

ABSTRACT

Cell apoptosis is common after infection with porcine reproductive and respiratory syndrome virus (PRRSV). PRRSV GP5 has been reported to induce cell apoptosis. To further understand the role of GP5 in PRRSV induced cell apoptosis, we established Marc-145 cell lines stably expressing full-length GP5, GP5$^{\Delta 84\text{-}96}$ (aa 84-96 deletion), and GP5$^{\Delta 97\text{-}119}$ (aa 97-119 deletion). Cell proliferation, cell cycle progression, cell apoptosis and virus replication in these cell lines were evaluated. Neither truncated nor full-length GP5 induced cell apoptosis in Marc-145 cells. However, GP5$^{\Delta 97\text{-}119}$, but not full-length or GP5$^{\Delta 84\text{-}96}$, induced a cell cycle arrest at the G2/M phase resulting in a reduction in the growth of Marc-145 cells. Additionally, GP5$^{\Delta 84\text{-}96}$ inhibited the replication of PRRSV in Marc-145 cells through induction of IFN-β. These findings suggest that PRRSV GP5 is not responsible for inducing cell apoptosis in Marc-145 cells under these experimental conditions; however it has other important roles in virus/host cell biology.

Introduction

Porcine reproductive and respiratory syndrome virus (PRRSV) is the causative agent of porcine reproductive and respiratory syndrome (PRRS), which has become one of the most economically significant swine diseases worldwide. PRRSV is an enveloped, positive-sense, single-stranded RNA virus. It belongs to the family of *Arteriviridae*, which also includes equine arteritis virus (EAV), lactate dehydrogenase-elevating virus (LDV), and simian hemorrhagic fever virus (SHFV) (Snijder and Meulenberg, 1998). PRRSV is further classified into two distinct genotypes, North American and European types, represented by the prototypes VR-2332 (Collins et al., 1992) and Lelystad virus (LV) (Wensvoort et al., 1991), respectively. In recent years, highly pathogenic PRRSV strains belonging to the North American genotype have emerged in China (Tian et al., 2007; Wang et al., 2012a).

The PRRSV genome is approximately 15 kb in length and contains 10 open reading frames (ORFs). ORF1a and ORF1b encode polyproteins that are processed into 14 non-structural proteins (nsp) by viral proteases (Fang and Snijder, 2010). ORF2a, ORF3 and ORF4 encode the glycosylated membrane associated minor structural proteins GP (2a), GP3 and GP4, respectively (Music and Gagnon, 2010). ORF2b encodes 2b protein, a non-glycosylated structural protein which is virion associated and the principal product of ORF2 (Wu et al., 2001). ORF5, ORF6 and ORF7 encode three major structural proteins, GP5, M and N protein, respectively. GP5a, referred to as ORF5a protein, is a novel structural protein encoded by an alternative ORF of the subgenomic mRNA encoding GP5 and is incorporated into the virion (Firth et al., 2011; Johnson et al., 2011).

* Corresponding author at: Department of Preventive Veterinary Medicine, College of Veterinary Medicine, Northwest A&F University, No. 22 Xinong Road, Yangling, Shaanxi 712100, China.
E-mail addresses: muyang@nwsuaf.edu.cn (Y. Mu), lifeiyang2007@126.com (L. Li), diana851218@163.com (B. Zhang), hbch228@163.com (B. Huang), jimingao2006@163.com (J. Gao), wangxiangpeng2003@126.com (X. Wang), wangchengbao@126.com (C. Wang), shqxiaojd@hotmail.com (S. Xiao), qinzhao_2004@sina.com (Q. Zhao), yanisun_2005@sina.com (Y. Sun), Zhanggaiping2003@yahoo.com.cn (G. Zhang), julian.hiscox@liverpool.ac.uk (J.A. Hiscox), zhouem@nwsuaf.edu.cn (E.-M. Zhou).

http://dx.doi.org/10.1016/j.virol.2015.05.019
0042-6822/

PRRSV has been reported to induce cell apoptosis both *in vivo* and *in vitro* (Choi and Chae, 2002; Kim et al., 2002; Lee and Kleiboeker, 2007; Miller and Fox, 2004; Sirinarumitr et al., 1998; Sur et al., 1998). GP5 was reported to be responsible for inducing cell apoptosis in BSC-40 cells (Fernandez et al., 2002; Suarez et al., 1996). In contrast, Lee et al. (2004) found that Hela cells stably expressing GP5 did not show evidence of apoptotic cell death and they speculated that the difference might be due to a histidine tag and an antigenic tag placed in the N-terminal of GP5 fusion constructs. Consistent with this report, Ma et al. (2013) demonstrated that none of the PRRSV structural proteins, including GP5, had the potential to cause apoptosis in Marc-145 cells, one of the few cell lines permissive for PRRSV. Rather, non-structural protein (nsp) 2 and nsp4 played causative roles in PRRSV-induced apoptosis in Marc-145 cells. Nsp2 was also shown to accelerate PRRSV replication in Marc-145 cells (Wang et al., 2012b). Thus, the definitive role of GP5 in PRRSV induced cell apoptosis remains largely unknown.

GP5 is approximately 200 amino acids (aa) with an apparent molecular mass of 25 kDa (Dea et al., 2000; Gagnon et al., 2003). The protein consists of three transmembrane domains (TMs) and a hydrophilic C terminus of approximately 70 amino acids (Dokland, 2010; Thaa et al., 2013; Wissink et al., 2003; Zaulet et al., 2012) and plays critical roles in virus assembly, invasion and immune response of PRRSV (Liu et al., 2013; Plagemann, 2004a; Van Breedam et al., 2010; Wissink et al., 2005). A sequence, ^{37}SHLQLIYNL, in the first ectodomain of VR2332 was found to be the primary GP5 neutralization epitope and the substitutions of ^{42}I to T and ^{38}HL to TY blocked the recognition of antibodies to this epitope (Plagemann, 2004b). Fernandez et al. (2002) suggested that the first 119 amino acids constituted a region capable of fully inducing apoptosis. In the present study, three recombinant plasmids, designated pPB-GP5 (full-length GP5), pPB-GP5$^{\Delta 84\text{-}96}$ (truncated GP5 with a deletion of aa 84-96), and pPB-GP5$^{\Delta 97\text{-}119}$ (truncated GP5 with a deletion of aa 97-119), were constructed and transfected into Marc-145 cells to generate the corresponding Marc-145-GP5, Marc-145-GP5$^{\Delta 84\text{-}96}$ and Marc-145-GP5$^{\Delta 97\text{-}119}$ cell lines (Fig. 1). The selected deletion region of aa 84-119 covers the second ectodomain region of GP5 in which aa 90-119 was included. The cell proliferation, cell cycle progression, cell apoptosis and PRRSV replication in these cells were analyzed. Cellular apoptosis assays indicated that expression of either full-length GP5 or truncated GP5s of PRRSV strain SD16 in Marc-145 cells were incapable of inducing cell apoptosis. Stable expression of full-length GP5 or GP5$^{\Delta 84\text{-}96}$ had no effect on cell proliferation and cell cycle progression. However, expression of GP5$^{\Delta 97\text{-}119}$ inhibited Marc-145 cells growth by inducing cell cycle arrest in the G2/M phase. Viral replication was reduced in Marc-145-GP5$^{\Delta 84\text{-}96}$ cells infected with PRRSV and this corresponded with increased interferon (IFN) expression. These findings provided novel information regarding the role of PRRSV GP5 in PRRSV pathogenesis.

Results

Generation, characterization and validation of GP5, GP5$^{\Delta 84\text{-}96}$ and GP5$^{\Delta 97\text{-}119}$ stably expressing cell lines

Marc-145 cells were co-transfected with the donor plasmids pPB-GP5, pPB-GP5$^{\Delta 84\text{-}96}$, pPB-GP5$^{\Delta 97\text{-}119}$, or pPB and the helper plasmid, then the transfected cells were screened and cloned. The positive recombinant cell lines were obtained after four weeks puromycin selection and three times subcloning. These cells showed epithelial-like morphology (Fig. 2A) and the specific RT-PCR products were observed from Marc-145-GP5 (603 bp), Marc-145-GP5$^{\Delta 84\text{-}96}$ (564 bp), and Marc-145-GP5$^{\Delta 97\text{-}119}$ (534 bp) cells, while no PCR product was observed from Marc-145-GFP cells (Fig. 2B). The protein expression levels of GP5, GP5$^{\Delta 84\text{-}96}$ and GP5$^{\Delta 97\text{-}119}$ in their designated cell lines were confirmed by Western blot (Fig. 2C). The Western blot results showed two bands which are consistent with what would be expected for the different glycosylated forms of GP5 (Dea et al., 2000; Gagnon et al., 2003). Confocal microscopy indicated that GP5 and both truncated variations of GP5 localized mainly in the cytoplasm of the cells (date not shown). These results suggested that ORF5 and both truncated forms of ORF5 were stably integrated into genome of Marc-145 cells and subsequently expressed within the cells as a stable protein.

Cell proliferation is slowed in Marc-145-GP5$^{\Delta 97\text{-}119}$ cells

Growth of Marc-145-GP5, Marc-145-GP5$^{\Delta 84\text{-}96}$ and Marc-145-GFP cell lines was similar to that of their parental Marc-145 cell line as shown in Fig. 3A and cell proliferation increased rapidly at 48–96 h. However, Marc-145-GP5$^{\Delta 97\text{-}119}$ cells proliferated significantly slowly compared to Marc-145 cell line ($p < 0.05$). This was further confirmed by the population doubling time (PDT) of those cell lines. There was no difference in PDT of Marc-145-GP5, Marc-145-GP5$^{\Delta 84\text{-}96}$, Marc-145-GFP and Marc-145 at 48 h, 72 h, 96 h, and 120 h, but PDT of Marc-145-GP5$^{\Delta 97\text{-}119}$ increased significantly at 72 h, 96 h, and 120 h (Fig. 3B). Overall, Marc-145-GP5$^{\Delta 97\text{-}119}$ displayed slower proliferation activity. Each cell line was cultured for 60 passages in the absence of puromycin without obvious changes to the protein expression levels (data not shown).

Expression of GP5$^{\Delta 97\text{-}119}$ protein induces cell cycle arrest at the G2/M phase

The possible reason of the growth retardation of Marc-145-GP5$^{\Delta 97\text{-}119}$ cells was examined by flow cytometry analysis. The results showed that the G2/M phase cell numbers of Marc-145-GP5$^{\Delta 97\text{-}119}$ cells were significantly higher than those of other cell lines (Fig. 4).

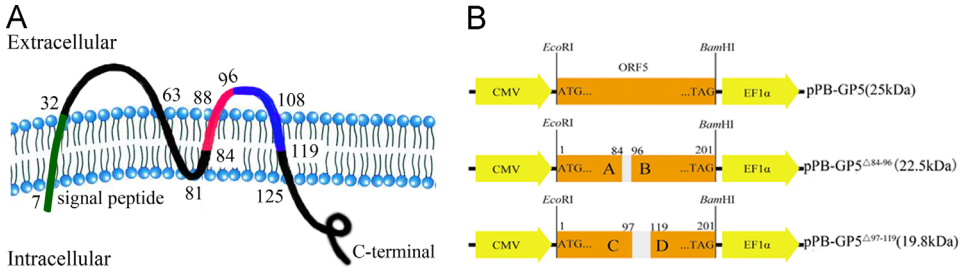

Fig. 1. Predicted PRRSV SD16 GP5 transmembrane structure and plasmid construction. (A) The transmembrane regions of PRRSV SD16 GP5 were predicted according to its full length sequence. The amino acid sequences are divided into a signal peptide region (aa 1 to 32), and the mature chain region (aa 33 to 200). The mature chain contains three transmembrane (TM) elements (TM1 from aa 64 to 80, TM2 from aa 82 to 88, and TM3 from aa 109 to 124). (B) The constructed plasmids that express GP5 or truncated GP5. Fragments A, B, C and D were amplified from full length ORF5 fragment and then fusions of A and B, or C and D were amplified using PCR. Recombinant plasmids, pPB-GP5 (expressing the full length GP5 of PRRSV SD16), pPB-GP5$^{\Delta 84\text{-}96}$ (expressing truncated GP5 with a deletion of aa 84-96), and pPB-GP5$^{\Delta 97\text{-}119}$ (expressing truncated GP5 with a deletion of aa 97-119), were constructed by inserting the target gene fragments into the PB transposon vector. The blank areas represent the deleted segments.

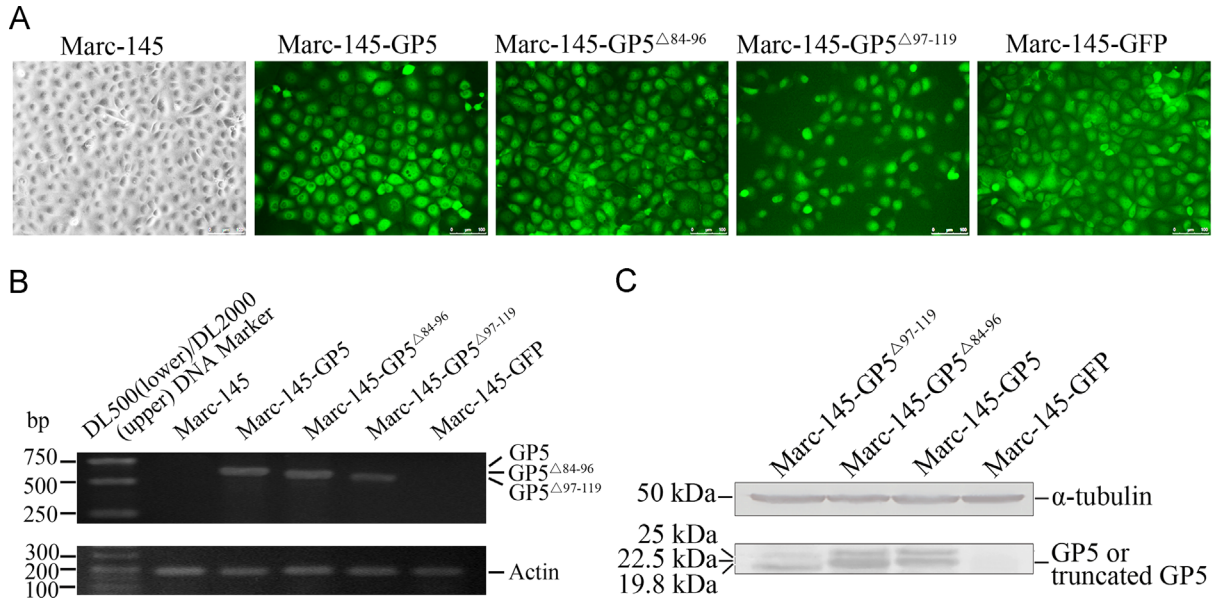

Fig. 2. Characterization and validation of RNA and protein expression in Marc-145-GP5, Marc-145-GP5$^{\Delta 84\text{-}96}$, Marc-145-GP5$^{\Delta 97\text{-}119}$, and Marc-145-GFP cells. (A) Epithelial-like cell morphology of the GP5 expressing cell lines was observed under microscope (200 ×). (B) Identification of exogenous gene expression in the novel cell lines with RT-PCR. Genomic RNA was extracted from the four cell lines and the target genes were amplified by RT-PCR with primers of GP5$^{1\text{-}83}$-F and GP5$^{97\text{-}201}$-R. Actin was used as internal control. (C) Western blot analysis of GP5 and truncated GP5 (GP5$^{\Delta 84\text{-}96}$ and GP5$^{\Delta 97\text{-}119}$) expression in Marc-145 cells (48 h) using anti-GP5 or α-tubulin primary antibodies.

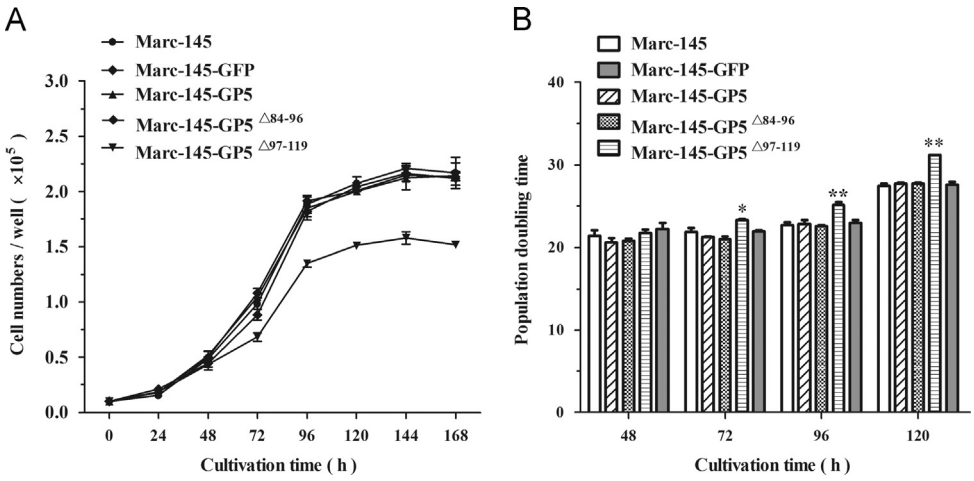

Fig. 3. Growth curves and PDT of Marc-145 cells expressing GP5 or truncated GP5. (A) Growth of Marc-145-GP5, Marc-145-GP5$^{\Delta 84\text{-}96}$, Marc-145-GP5$^{\Delta 97\text{-}119}$, and Marc-145-GFP cell lines. The data are mean ± SD of three independent experiments. (B) The PDT of those cell lines were determined at 48 h, 72 h, 96 h, 120 h after seeding according to the formula: PDT = [lg 2/(lg N_t − lg N_0)] × t where N_t = number of cells after t hours of culturing and N_0 = number of cells seeded.

Expression of GP5 or truncated GP5 of PRRSV strain SD16 does not induce cell apoptosis

The apoptotic indexes (AI) of Marc-145-GP5, Marc-145-GP5$^{\Delta 84\text{-}96}$, Marc-145-GP5$^{\Delta 97\text{-}119}$ and Marc-145-GFP were calculated according to the ratio between the expression of Bax and Bcl-2. As shown in Fig. 5A, in Marc-145 cells infected with PRRSV SD16 at 1 MOI, the apoptotic indexes were 0.37 ± 0.03 at 24 h, 1.36 ± 0.03 at 48 h, and 2.96 ± 0.09 at 72 h postinfection. The apoptotic indexes for Marc-145-GP5, Marc-145-GP5$^{\Delta 84\text{-}96}$, Marc-145-GP5$^{\Delta 97\text{-}119}$ and Marc-145-GFP cells after 24 h in culture were 0.71 ± 0.06, 0.70 ± 0.04, 0.91 ± 0.01, and 0.70 ± 0.17, respectively. All cell lines showed a decrease in apoptotic index compared to control cells. Although the apoptotic indices of all cell lines changed to varying degrees when continuing cell culture to 72 h, Marc-145 cells infected with PRRSV SD16 were the only cells to show a significant increase in apoptotic index. To further confirm whether stably expressed GP5 or truncated GP5 induces cell apoptosis, the cleaved caspase-3 was detected by Western blot. The cleaved caspase-3 (approximately 17 kDa) was only detected in Marc-145 cells infected with PRRSV SD16 at 1 MOI but not from un-infected Marc-145, Marc-145-GP5, Marc-145-GP5$^{\Delta 84\text{-}96}$, Marc-145-GP5$^{\Delta 97\text{-}119}$ or Marc-145-GFP cell lines cultured to 72 h (Fig. 5B). Additionally, DNA degradation into oligonucleotide fragments showing cell apoptosis was detected by agarose gel electrophoresis. The results revealed that DNA fragmentation was observed only in Marc-145 cells infected with PRRSV SD16, but not in other cell lines (Fig. 5C). Furthermore, when the cell lines were treated with the Apoptosis Inducers (Beyotime, China) or infected with PRRSV SD16, the cleaved caspase-3 was detected from all cell lines which indicated these cell lines were equally susceptible (Figs. 5D and S3). Together, these data indicate that the expression of GP5 or truncated GP5 of PRRSV strain SD16 did not induce cell apoptosis in Marc-145 cells.

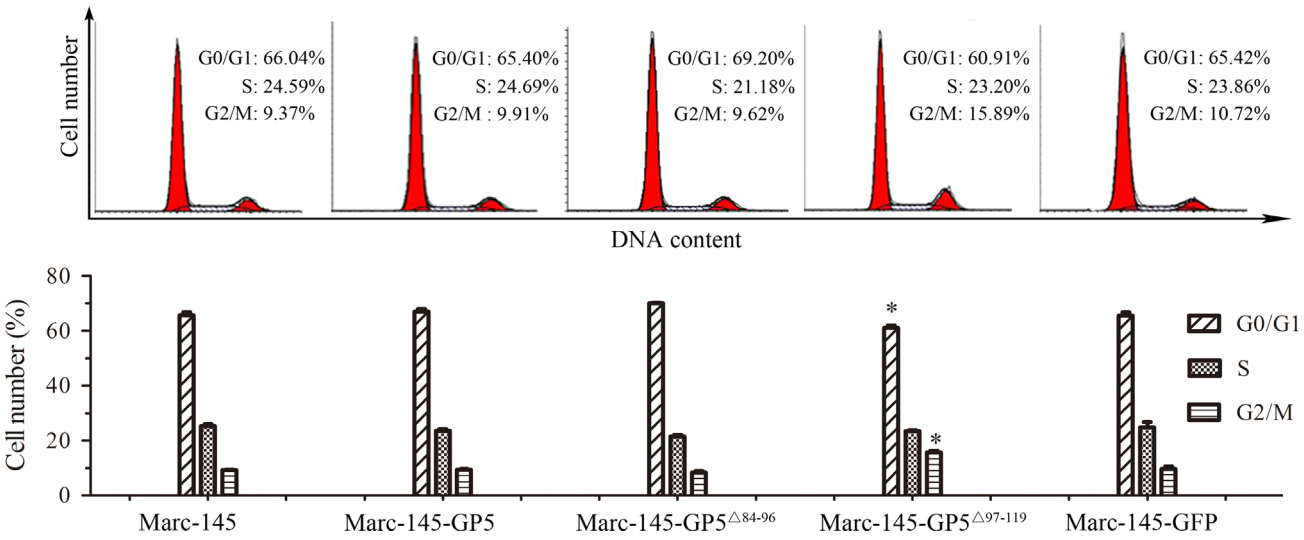

Fig. 4. Expression of PRRSV GP5$^{\Delta 97\text{-}119}$ in Marc-145 induces cell cycle arrest at the G2/M phase. Flow cytometry analysis of cell cycle using PI staining. Cell numbers shown in the top row are representative of one of three independent experiments. The results represented in the bottom row of graphs are mean ± SD from three independent experiments. $^{*}p < 0.05$ *versus* that of Marc-145 control cells.

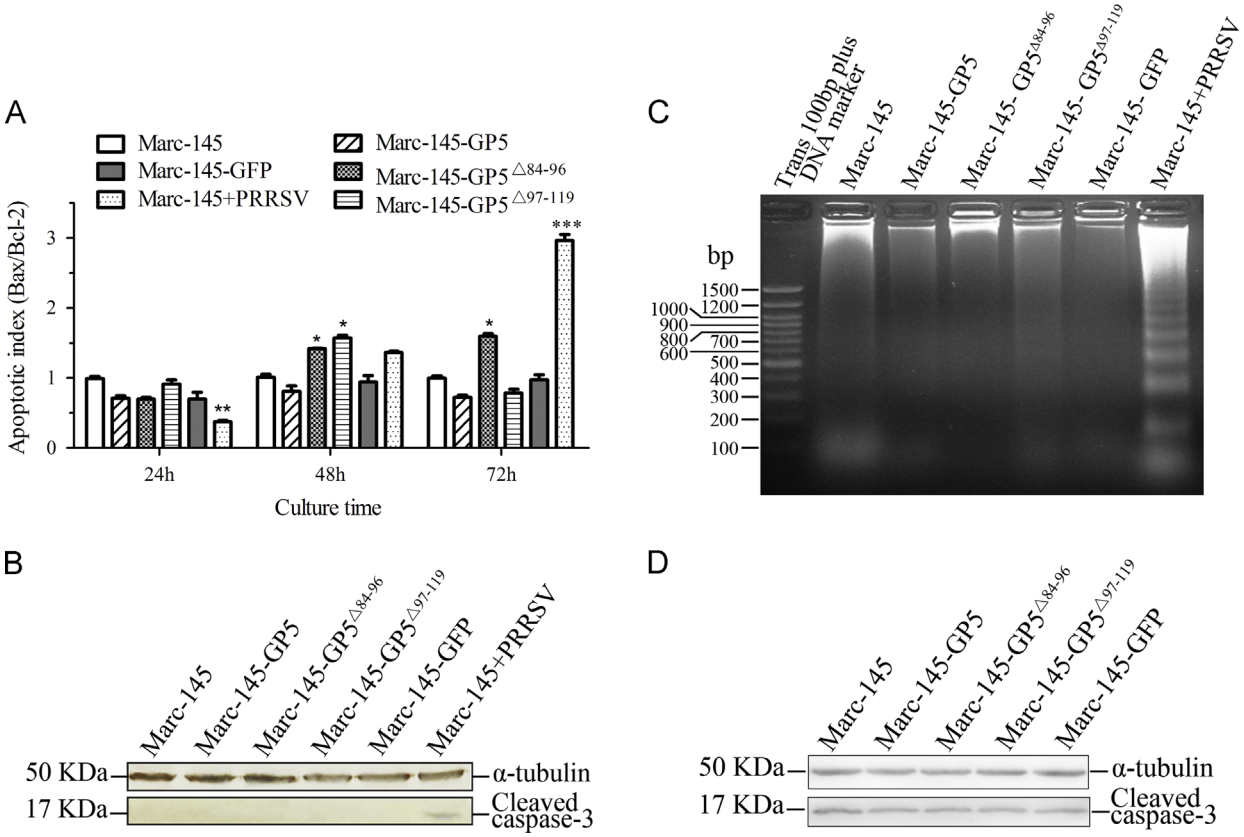

Fig. 5. Stable expression of PRRSV GP5 or truncated GP5s does not induce apoptosis in Marc-145 cells. Un-infected Marc-145 cells were used as a negative control and Marc-145 cells infected with PRRSV SD16 at 1 MOI were used as positive control for apoptosis. (A) Apoptotic indexes (AI) of Marc-145-GP5, Marc-145-GP5$^{\Delta 84\text{-}96}$, Marc-145-GP5$^{\Delta 97\text{-}119}$ and Marc-145-GFP were calculated according to Bax/Bcl-2 relative expression level. The results are mean ± SD from three independent experiments. (B) Cleaved caspase-3 activity was analyzed by Western blot. Cells were collected and lysed after culture 72 h. The presence of cleaved caspase-3 (17 kDa) was analyzed using Western blot with α-tubulin as an internal reference. (C) DNA fragmentation was detected using agarose gel electrophoresis. All cell lines as well as Marc-145 control cells were cultured for 72 h and DNA was extracted to further analyze DNA fragmentation. (D) The cleaved caspase-3 was detected from all cell lines induced by Apoptosis Inducer.

Expression of GP5$^{\Delta 84\text{-}96}$ inhibits PRRSV replication in Marc-145 cells

To determine the influence of GP5 or truncated GP5 expression on PRRSV replication, all cell lines were infected with PRRSV strain SD16 at 1 MOI and cells were collected at 24 h, 36 h, 48 h, 60 h and 72 h after infection. PRRSV N gene copy numbers in each cell line were quantified using qRT-PCR. The N gene copy numbers in Marc-145-GP5$^{\Delta 84\text{-}96}$ cells decreased significantly from 24 h to 72 h in comparison to those in Marc-145 cells ($p < 0.001$, Table 2). In addition, PRRSV replication was lower in Marc-145-GP5$^{\Delta 84\text{-}96}$ cells at all time points assessed than that in other cell lines by measuring virus titers in the cell culture supernatant. At 36 h post-infection, the virus titer in

Marc-145 cells was $10^{6.21}$ $TCID_{50}$/mL, but in Marc-145-GP5$^{\Delta 84\text{-}96}$ cells it was only $10^{3.92}$ $TCID_{50}$/mL (Table 2).

Western blot analysis of the abundance of the N protein at 36 h post-infection showed that the level of N protein expression was lower in Marc-145-GP5$^{\Delta 84\text{-}96}$ than that in other cell lines with α-tubulin expression remained constant (Fig. 6). The observation of CPE and an IFA analysis of the PSSRV N protein expression at 36 h post-infection also supported that PRRSV replication was inhibited in Marc-145-GP5$^{\Delta 84\text{-}96}$ cells (Fig. S1).

Expression of GP5$^{\Delta 84\text{-}96}$ inhibits the replication of several PRRSV strains in Marc-145 cells

To determine whether the inhibition of PRRSV replication in Marc-145 GP5$^{\Delta 84\text{-}96}$ cells is strain specific, these cells were further infected with PRRSV strains VR-2332 and JXA1. The appearance of CPE and the results of IFA for N protein expression at 36 h post-infection indicated that the replication of these PRRSV strains was also inhibited to some degree in Marc-145-GP5$^{\Delta 84\text{-}96}$ cell line (Fig. S2A). However, only the replication of SD16 was inhibited significantly (4.13 ± 0.10 in Marc-145-GP5$^{\Delta 84\text{-}96}$ VS 5.29 ± 0.26 in Marc-145-GFP, $p = 0.0039$), shown by detection of virus titers in the supernatant at 48 h post-infection (Fig. S2B).

Expression of GP5$^{\Delta 84\text{-}96}$ induces interferon expression in Marc-145 cells

The relative expression of IFN-α, β and γ was quantified with qRT-PCR using the $2^{-\Delta\Delta Ct}$ method. The results showed a 2-fold increase of IFN-β mRNA expression levels in Marc-145-GP5$^{\Delta 84\text{-}96}$ cells than that in Marc-145cells (Fig. 7A). However, after infected with PRRSV SD16 for 48 h, the relative mRNA expression levels of IFN-α and IFN-β were increased 3-fold and 148-fold, respectively, in Marc-145-GP5$^{\Delta 84\text{-}96}$ than that in Marc-145 cells (Fig. 7B). The increase of IFN-β mRNA levels was also detected in Marc-145-GP5$^{\Delta 84\text{-}96}$ cells infected with PRRSV strains VR-2332 or JXA1 (Fig. 7C). Collectively, these data suggest that IFN-α and IFN-β up-regulation may be responsible for the inhibition of replication of PRRSV in Marc-145 GP5$^{\Delta 84\text{-}96}$ cells.

Discussion

The underlying mechanism of PRRSV infection is poorly understood. In this study, we investigated the role of PRRSV GP5 and truncated GP5 with aa 84-96 and aa 97-119 deletion in cell apoptosis, cell cycle progression, and PRRSV proliferation. Our results demonstrated that PRRSV strain SD16 GP5 or truncated GP5s could not induce apoptosis in Marc-145 cells. Additionally, we confirmed that PRRSV GP5 plays a positive role in PRRSV replication, and further study showed that the intracellular region of aa 84-96 in GP5 was important for virus infection.

Increasing amounts of evidence indicate that viral infection and the expression of viral proteins cause the host cell to arrest at certain phase to create a favorable environment for viral replication and progeny virus production (Dove et al., 2006; Xu et al., 2005; Zhao and Elder, 2005). Avian reovirus (ARV) infection and ARV p17 transfection resulted in the accumulation of infected and/or transfected cells in the G(2)/M phase of the cell cycle (Chulu et al., 2010). HIV Vpr protein induces cell cycle arrest in the G2/M phase and is thought to benefit viral proliferation by providing an optimized cellular environment and a blockade against the host immune responses (Li et al., 2010). In this research, the overall growth kinetics of Marc-145-GP5, Marc-145-GP5$^{\Delta 84\text{-}96}$ and Marc-145-GFPcell lines were similar to that of their parental Marc-145 cells; however, Marc-145-GP5$^{\Delta 97\text{-}119}$ cells proliferated more slowly than the other cell lines with the fact that Marc-145-GP5$^{\Delta 97\text{-}119}$ cell line had significantly more cells in the G2/M phase compared to the Marc-145 and Marc-145-GFP cell lines. These results indicate that the slower proliferation of Marc-145-GP5$^{\Delta 97\text{-}119}$ is caused by inducing cell cycle arrest at the G2/M phase.

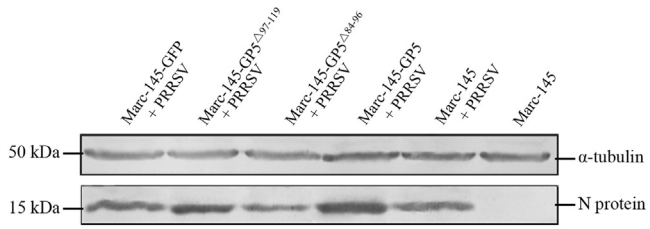

Fig. 6. N protein expression was upregulated in Marc-145-GP5 cells and reduced in Marc-145-GP5$^{\Delta 84\text{-}96}$ cells. PRRSV SD16 N protein expression in Marc-145 cell lines was detected at 36 h post-infection via Western blot using anti-PRRSV nucleocapsid (N) antibody 6D10, with α-tubulin as an internal reference.

Apoptosis has been proposed as an immediate host defense response upon viral infections, or it may serve as a viral pathogenic strategy to maximize virus progeny. PRRSV infection can induce cell apoptosis in alveolar macrophages, porcine intravascular monocytes, lymphocytes and testicular germ cells of infected pigs, which corresponds to a sharp reduction in these cell numbers in PRRSV positive swine (Costers et al., 2008; Gomez-Laguna et al., 2013; Sirinarumitr et al., 1998; Suarez, 2000; Sur et al., 1997). Using GP5 expressed by a recombinant vaccinia virus, GP5 was reported to be responsible for apoptosis induced by PRRSV infection (Fernandez et al., 2002; Suarez et al., 1996). However, these findings have not been supported by subsequent work. Lee et al. (2004) showed that GP5 could not induce apoptosis, and speculated that the difference might be due to a histidine tag and an antigenic tag placed in the N-terminal of GP5 fusion constructs. Using pcDNA3.1(+) vector to transfect Marc-145 cells, it was found that none of the PRRSV structural proteins, including GP5, had the potential to cause apoptosis (Ma et al., 2013). In our study, PiggyBac™ Transposon Vector System in which the exogenous genes expressed in the transposed cells are independent was used (Wang et al., 2013). Our findings were consistent with that of Lee et al. (2004) and Ma et al. (2013), showing that full length or truncated GP5 does not cause apoptosis when stably expressed in Marc-145 cells.

Bcl-2 is an important proto-oncogene which was the first gene implicated in the regulation of apoptosis. Its protein is able to prevent apoptosis, facilitating cell survival independent of promoting cell division. Bax (Bcl2-associated X protein) is the most characterized death-promoting member of the Bcl-2 family. Apoptosis tendency can be estimated by an apoptotic index (AI) which can be represented by the ratio between Bax/Bcl-2 expression (Amaral et al., 2011; Salakou et al., 2007). Samples with AI higher than 1 were regarded as having higher apoptotic activity than samples exhibiting an AI lower than 1. In this study, although the apoptotic indices of the cell lines changed to varying degrees when continuing culture to 72 h, the only significant increase was in Marc-145 cells infected with PRRSV SD16 (Fig. 5A). This suggested that PRRSV infection induced an apoptotic tendency in Marc-145 cells, but stable expression of PRRSV GP5 or truncated GP5s in Marc-145 cells alone did not induce this tendency.

PRRSV has been reported to induce apoptosis through caspase-mediated pathways (Lee and Kleiboeker, 2007). Signal cascades activated by the extrinsic and intrinsic pathways converge on caspase-3 which is one of the executioner caspases. Our study confirmed that cleaved caspase-3 could not be detected in Marc-145, Marc-145-GP5, Marc-145-GP5$^{\Delta 84\text{-}96}$, Marc-145-GP5$^{\Delta 97\text{-}119}$ and Marc-145-GFP cells at time points up to 72 h in culture (Fig. 5B). Electrophoresis results also revealed that no typical changes in DNA fragmentation were observed in the lanes of Marc-145, Marc-145-GP5, Marc-145-GP5$^{\Delta 84\text{-}96}$, Marc-145-GP5$^{\Delta 97\text{-}119}$, and Marc-145-GFP cells, showing that GP5 and truncated GP5s could not induce the

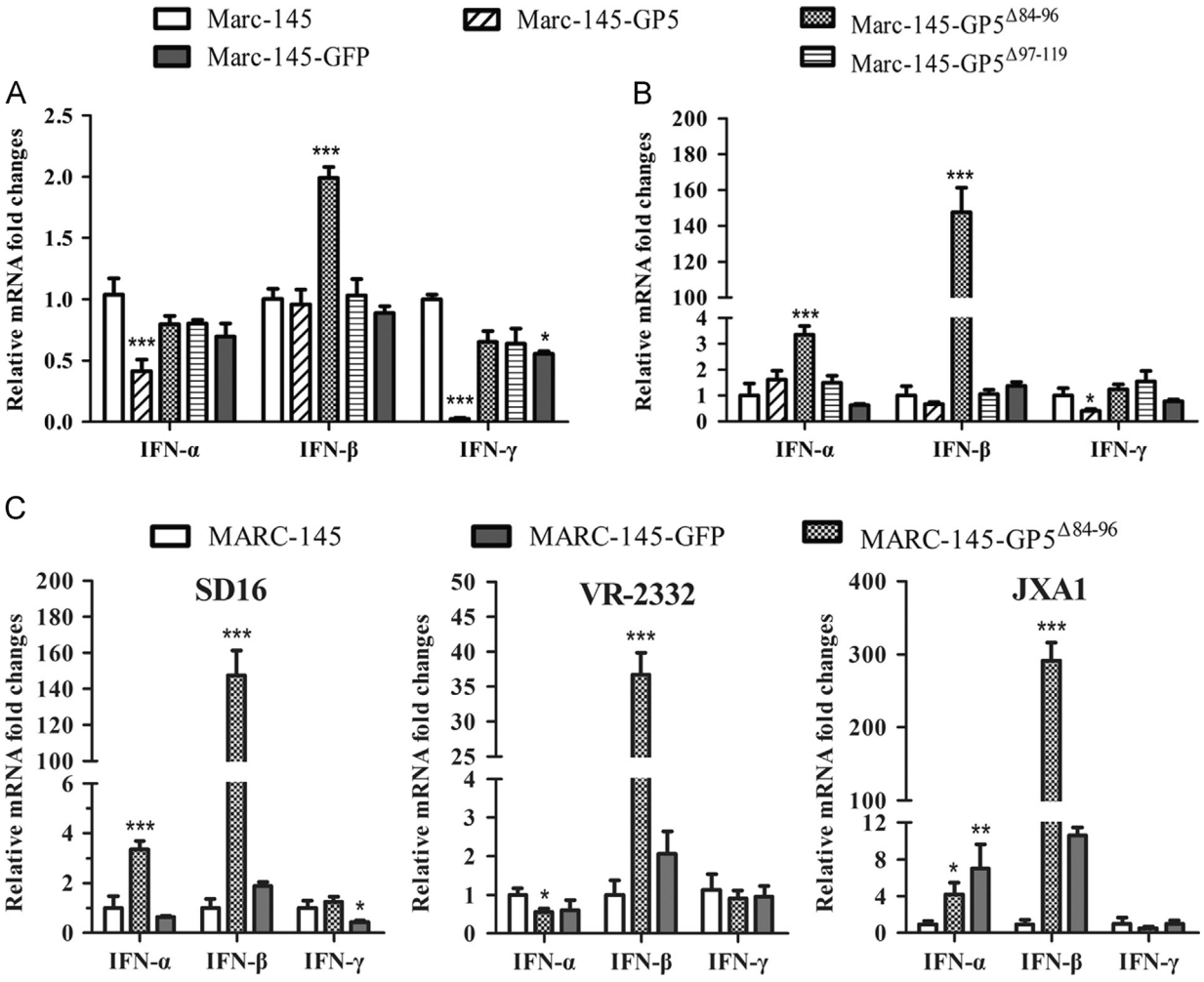

Fig. 7. Quantification of INF levels in Marc-145 cell lines after PRRSV infection. The transcriptional level of IFN-α, IFN-β and IFN-γ was assessed by qRT-PCR. Relative quantities of mRNA accumulation were evaluated using the $2^{-\Delta\Delta Ct}$ method, and the relative fold change of each IFN gene expression was then calculated between the novel cell lines and parental control Marc-145 cells. Data are representative of the mean values from three independent experiments and error bars represent standard deviations. All values are normalized to β-actin. (A) Relative expression of IFN mRNAs in Marc-145-GP5, Marc-145-GP5$^{\Delta 84\text{-}96}$, Marc-145-GP5$^{\Delta 97\text{-}119}$ and Marc-145-GFP. (B) Relative expression of IFN mRNAs in Marc-145-GP5, Marc-145-GP5$^{\Delta 84\text{-}96}$, Marc-145-GP5$^{\Delta 97\text{-}119}$ and Marc-145-GFP 48 h after PRRSV SD16 infection. (C) Relative expression of IFNs in Marc-145-GP5$^{\Delta 84\text{-}96}$ 48 h after PRRSV SD16, VR-2332, or JXA1 infection. $^{*}p < 0.05$, $^{**}p < 0.01$, and $^{***}p < 0.001$ *versus* control group.

degradation of DNA into fragments (Fig. 5C). However Marc-145 cells infected with PRRSV SD16 did exhibit DNA fragmentation. When those cell lines were treated with Apoptosis Inducer for 18 h, the cleaved caspase-3 was detected from all cell lines indicating that insertion of the vector system gene did not affect the apoptotic system of the cell lines (Fig. 5D). When these cells lines were infected with PRRSV SD16 strain at 1 MOI for 60 h, the cleaved caspase-3 was increased in Marc-145-GP5$^{\Delta 84\text{-}96}$ (Fig. S3), which may be due to that GP5$^{\Delta 84\text{-}96}$ expression inhibited PRRSV replication and after 60 h infection, more cells were in apoptosis; in contrast, most cells of other cell lines had died. This collective data suggests that expression of PRRSV strain SD16 GP5 or truncated GP5s does not induce apoptosis in Marc-145 cells.

GP5 plays critical roles in the assembly, invasion and immune response of the PRRSV particle (Liu et al., 2013; Wissink et al., 2005). Using our GP5 expressing Marc-145 cell lines, we investigated possible changes in virus replication. PRRSV N gene copy numbers in Marc-145-GP5$^{\Delta 84\text{-}96}$ decreased significantly compared to Marc-145 cells at all-time points analyzed. The viral titers demonstrated that PRRSV replicated more slowly in Marc-145-GP5$^{\Delta 84\text{-}96}$ at all-time points, and more rapidly in Marc-145-GP5, compared to control cells at early stages after PRRSV infection (Table 2). Western blot analysis showed that N protein expression increased in Marc-145-GP5 and decreased in Marc-145-GP5$^{\Delta 84\text{-}96}$ at 36 h post-infection (Fig. 6). The appearance of specific CPEs, and IFA analysis of N protein expression at 36 h post-infection, further confirmed that PRRSV SD16 replication was inhibited in Marc-145-GP5$^{\Delta 84\text{-}96}$ cells (Figs. S1 and S2). When Marc-145-GP5$^{\Delta 84\text{-}96}$ cells were infected with PRRSV VR-2332, or JXA1, the appearance of CPE, and IFA analysis of N protein expression at 36 h post-infection (Fig. S2B), again indicated that expression of GP5$^{\Delta 84\text{-}96}$ could inhibit PRRSV replication in a non-strain specific manner.

The region consisting of aa 84-119 includes the second extracellular region and parts of the intracellular region of GP5 (Fig. 1). Dea et al. (2000) shows that GP5 possesses two to four potential N-linked glycosylation sites that are located in a small ectodomain, and Wei et al. (2012) found that N-linked glycosylation of GP5 was critically important for virus replication *in vivo*. In our Marc-145-GP5$^{\Delta 84\text{-}96}$ cell line, PRRSV replication was inhibited significantly, but in our Marc-145-GP5$^{\Delta 97\text{-}119}$ cell line, the influence on PRRSV replication was not obvious (Table 2). We speculate that there are some key sites in the region of aa 84-96 specifically that have an important influence on virus replication. Further studies are needed to elucidate this problem.

Previous studies have demonstrated that IFN-α, β and γ have an antiviral effect against PRRSV (Bautista and Molitor, 1999; Luo et al., 2011; Overend et al., 2007; Yang et al., 2013). Consistent with

this, in the present study, a 2-fold increase of IFN-β mRNA expression was detected in Marc-145-GP5$^{\Delta 84\text{-}96}$ cells (Fig. 7A) and after PRRSV strain SD16 infection IFN-α and IFN-β expression levels were increased 3-fold and 148-fold, respectively (Fig. 7B). This effect was not specific to viral strain and was replicated following infection with VR-2332 or JXA1. In each case, interferon expression, especially IFN-β expression, was up-regulated significantly (Fig. 7C). These findings suggest that stable expression of GP5$^{\Delta 84\text{-}96}$ may inhibit PRRSV replication by up-regulating interferon. However, more studies are required to further examine the induction of cytokines and their role in PRRSV replication in Marc-145-GP5$^{\Delta 84\text{-}96}$ cells.

In summary, our results show that the stable expression of GP5 or truncated GP5s (GP5$^{\Delta 84\text{-}96}$ or GP5$^{\Delta 97\text{-}119}$) of PRRSV strain SD16 did not induce apoptosis in Marc-145 cells. However, each truncated form of GP5 was shown to have unique effects on Marc-145 cells. Stable expression of PRRSV GP5$^{\Delta 97\text{-}119}$ inhibits Marc-145 cell growth by inducing cell cycle arrest at G2/M phase. Expression of GP5$^{\Delta 84\text{-}96}$ can inhibit replication of multiple strains of PRRSV in Marc-145 cells. This inhibition may be induced by up-regulating interferons, particularly IFN-β. This study provides novel insight into the function of the PRRSV GP5 protein which will be helpful for further understanding the molecular mechanisms of PRRSV pathogenesis.

Materials and methods

Cell lines, viruses and antibodies

Marc-145 cells were purchased from the China Center for Type Culture Collection (CCTCC) and cultured in Dulbecco's Modified Eagle's Medium (DMEM) with high glucose (Life Technologies Corporation, USA) supplemented with 10% fetal bovine serum (FBS) (Gibco BRL, USA) and 1% antibiotics-antimycotic (Life Technologies Corporation, USA). The PRRSV strains used were VR-2332 (GenBank: EF536003.1) and two highly pathogenic PRRSV isolates of SD16 (GenBank: JX087437.1) and JXA1 (GenBank: EF112445.1). These viruses were propagated and titrated in Marc-145 cells. A monoclonal anti-PRRSV nucleocapsid (N) antibody 6D10, anti-GP5 mouse serum and anti-PRRSV swine serum were prepared in our laboratory. Anti-α-tubulin antibody was purchased from Sigma-Aldrich (St. Louis, MO). Horseradish peroxidase (HRP)-conjugated goat anti-mouse IgG, HRP-conjugated goat anti-rabbit IgG, Texas Red-affiniPure goat anti-swine IgG (H+L), and Texas Red-affiniPure goat anti-mouse IgG (H+L) were purchased from Jackson ImmunoReseach (West Grove, PA).

Plasmid construction

Total RNA was extracted from PRRSV SD16 using High Pure Viral RNA Kit (Roche, Swit.) and the full length ORF5 fragment was amplified (primers are listed in Table 1). As shown in Fig. 1B, fragments A, B, C and D were amplified from full length ORF5 fragment and then fusions of A and B, or C and D were amplified using overlap PCR. Three recombinant plasmids, pPB-GP5 (expressing full length GP5 of PRRSV SD16), pPB-GP5$^{\Delta 84\text{-}96}$ (expressing a truncated GP5 with a deletion of aa 84-96), and pPB-GP5$^{\Delta 97\text{-}119}$ (expressing a truncated GP5 with a deletion of aa 97-119), were constructed by inserting the targeted gene fragments into the site between *Eco*R I and *Bam*H I restriction enzyme sites of a PB transposon vector of PiggyBac Transposon System Vectors (System Biosciences, USA) and confirmed by sequence analysis (Sangon Biotech, China).

Table 1
Primers used to amplify different gene fragments.

Primer name	Sequence (5′–3′)
GP5-F	CGGAATTCATGTTGGGGAAGTGCTTGACC(*Eco*R I)[a]
GP5-R	CGGGATCCCTAGAGACGACCCCATTGTTC(*Bam*H I)
GP5$^{1\text{-}83}$-F	ATGTTGGGGAAGTGCTTGACCG
GP5$^{1\text{-}83}$-R	CGTGATAATATCCGGCGGTGGAGGTGAGTGCCCCATAGGAAAC
GP5$^{97\text{-}201}$-F	TGTTTCCTATGGGGCACTCACCTCCACCGCCGGATATTATCAC
GP5$^{97\text{-}201}$-R	CTAGAGACGACCCCATTGTTCCGCT
GP5$^{1\text{-}96}$-R	CCTAATGACAAAGCAAATCAGCACAGTGGCCAGACCAACTGTG
GP5$^{120\text{-}201}$-F	CACAGTTGGTCTGGCCACTGTGCTGATTTGCTTTGTCATTAGG
ORF7-F	AGATCATCGCCCAACAAAAC
ORF7-R	GACACAATTGCCGCTCACTA
IFN-α-F	GGCACTGCCCTTTGCTTTAC
IFN-α-R	GTTATCCAGGCTGTGGGTCTCA
IFN-β-F	GCAATTGAATGGAAGGCTTGA
IFN-β-R	CAGCGTCCTCCTTCTGGAACT
IFN-γ-F	TGTCCAACGCAAAGCAGTACA
IFN-γ-R	ACCTCGAAACATCTGACTCCTTTT
Bax-F	ACCAAGAGGCTGAGCGAGTGT
Bax-R	TTGCTGGCAAAGTAGAAAAGGC
Bcl-2-F	GAGAAGGTGAGAAGCCCTGAGT
Bcl-2-R	GAGACAAGGTCAAAGGGACAAC
β-actin-F	CGGGAAATCGTGCGTGAC
β-actin-R	ATGCCCAGGAAGGAAGGTTG

[a] The underlined are *Eco*R I and *Bam*H I restriction enzyme sequences.

Generation of Marc-145 cell lines stably expressing GP5 or truncated GP5

The piggyBac^{TM} Transposon vector system (System Biosciences, USA) was applied to generate cell lines stably expressing GP5, GP5$^{\Delta 84\text{-}96}$, GP5$^{\Delta 97\text{-}119}$ or GFP in Marc-145 cells as described previously (Wang et al., 2013). Briefly, one day before transfection, Marc-145 cells were seeded in 6-well plates at a density of 2×10^5 cells/well. When cells reached 80% confluence, they were co-transfected with the donor plasmid and the helper plasmid using X-treme GENE HP DNA Transfection Reagent (Roche, Switzerland.) according to the manufacturer's instructions. Green fluorescence was observed at 24 h posttransfection. Transfected cells were cultured in fresh medium in the presence of puromycin (Merck, USA) at a concentration of 10 μg/mL for 48 h. Puromycin-selective medium was then replaced every second day. Puromycin-resistant and GFP-positive cell clones appeared after 10 days of puromycin selection. The single cell colonies were sub-cloned and saved as cell stocks. Cell clones were cultured in growth medium in the absence of puromycin to evaluate the stability of exogenous gene expression. This procedure was used to produce the four cell lines, (Marc-145-GP5, Marc-145-GP5$^{\Delta 84\text{-}96}$, Marc-145-GP5$^{\Delta 97\text{-}119}$, and Marc-145-GFP), which were used along with Marc-145 control cells in the following studies.

RT-PCR analysis

Transposed Marc-145-GP5, Marc-145-GP5$^{\Delta 84\text{-}96}$, Marc-145-GP5$^{\Delta 97\text{-}119}$, and Marc-145-GFP cell lines were examined by RT-PCR to determine the presence of the full length or truncated ORF5 gene as follows. 5×10^5 cells were collected and total RNA was extracted using RNAiso plus (Takara, Japan). RT-PCR was performed using 1 μg RNA and M-MLV reverse transcriptase (Takara, Japan) with GP5-F and GP5-R primers (Table 1) and analyzed on 1% agarose gel.

Western blot analysis

All recombinant cell lines were harvested and treated with NP40 lysis buffer (Beyotime, China), and then protein concentrations were determined using the Pierce BCA protein assay kit (Thermo, USA). Equal protein concentrations were loaded and electrophoresed on 12%

SDS-PAGE and then transferred to PVDF membranes (Millipore, USA) using BIO-RAD Mini Trans-blot. The membranes were blocked with 5% non-fat dry milk and then incubated with indicated primary antibodies overnight at 4 °C, followed by HRP-conjugated secondary antibodies. α-tubulin was used as a loading control. The protein bands were visualized using diaminobenzidine (DAB) as the substrate (Tiangen, China).

Confocal microscope analysis

The cells were seeded on slides at a density of 1×10^4 cells/slide and cultured 24 h, then fixed with 4% paraformaldehyde for 10 min at room temperature (RT), then washed with PBS and permeabilized with 0.3% triton X-100/PBS for 3 min, washed and then blocked with 5% Bovine Serum Albumin (BSA) in PBS. After washing, the cells were incubated with swine anti-PRRSV serum for 1 h at 37 °C, washed with PBS, and incubated with Texas Red-affiniPure goat anti-swine IgG (H+L). Finally, cells were counterstained with 4′, 6′-diamidino-2-phenylindole dihydrochloride (DAPI, Sigma), and visualized using confocal microscopy (Nikon A1R, Japan).

Indirect immunofluorescent assay (IFA)

The cells were seeded in 24-well plates and infected with PRRSV at a multiplicity of infection of 1 (1 MOI). Cytopathic effects (CPE) were observed daily as a qualitative measure of infection. Thirty-six hours following PRRSV infection, the cells were fixed with 4% paraformaldehyde for 10 min at RT, then washed with PBS and permeabilized with 0.3% triton X-100/PBS for 3 min, washed and then blocked with 5% BSA/PBS. After washing, the cells were incubated with anti-PRRSV nucleocapsid monoclonal antibody 6D10 for 1 h at 37 °C, washed with PBS and incubated with Texas Red-affiniPure goat anti-mouse IgG (H+L). Finally, cells were counterstained with DAPI, and visualized using Leica microsystems (Leica AF6000, Germany).

Growth curve plotting and population doubling time (PDT) determination

The growth curve plotting and population doubling time (PDT) determination for those cell lines were performed as previously described (Feng et al., 2013; Hong et al., 2007) with the following modifications. Marc-145-GP5, Marc-145-GP5$^{\Delta 84\text{-}96}$, Marc-145-GP5$^{\Delta 97\text{-}119}$, Marc-145-GFP and Marc-145 were seeded in 24-well plates at 1×10^4 cells/well. The cells in three wells were digested with trypsin each day for eight day, cell numbers were counted, and the growth curves were plotted based on the average cell numbers against culture time. PDT was calculated according the formula: $PDT = [\log 2/(\log N_t - \log N_0)] \times t$, where N_t = number of cells after t hours of culturing, N_0 = number of cells seeded.

Cell cycle analysis

Cell cycle was measured using propidium iodide (PI) staining method as previously described (Xu et al., 2013) with the following modifications. Briefly, 2×10^6 cells from each of the five cell lines were harvested and washed 2 times with PBS, then resuspended in 500 μL PBS and fixed for at least 1 h with 3 mL 70% cold ethanol. After centrifugation, cell pellets were washed with PBS and resuspended in 1 mL PI solution containing 50 μg/mL PI, 50 μg/mL RNase A, and 0.1% Triton X-100, then incubated at 4 °C for 30 min. The nuclear DNA content was analyzed by flow cytometry (Beckman Coulter Cytomics Altra, USA).

Quantitative real-time PCR (qRT-PCR)

Total RNA was extracted from cell samples using the High Pure Viral RNA Kit (Roche, Swit.) according to the manufacturer's instructions and cDNA was synthesized with the PrimeScript® RT reagent kit (TaKaRa, Japan). The primers for qRT-PCR are listed in Table 1. qRT-PCR analysis was performed with Step One Plus® real-time PCR system (Applied Biosystems, USA). β-actin was used as an internal control. Relative quantification of target genes expression was calculated with the $2^{-\Delta\Delta Ct}$ method.

DNA fragmentation assay

The cells were collected after 72 h in culture and were lysed in 200 μL lysis buffer (50 mM Tris, 20 mM EDTA, 1% NP-40, and 1 mg/mL proteinase K, pH 7.5) at 55 °C for 3 h. Then, RNase A was added to a final concentration of 0.5 mg/mL and incubated at 55 °C for 1 h. DNA was extracted with phenol/chloroform/isoamyl alcohol (25/24/1) and analyzed on 1.5% agarose gel. After electrophoresis, the gel was stained with ethidium bromide (Gibco BRL, Scotland) and the bands obtained were visualized using the gel imaging analysis system (Syngene, UK).

Analysis of PRRSV replication in Marc-145 cell lines

The cells were seeded in 24-well culture plates at a density of 5×10^4 cells/well, and cultured to reach approximately 80% confluence. PRRSV strains SD16, VR-2332, or JXA1 were used to infect the cells at a multiplicity of infection (MOI) of 1. Viral titers were determined in each of the 5 Marc-145 cell lines using 10-fold serial dilutions. The 50% tissue culture infective dose ($TCID_{50}$/mL) was calculated using the Reed–Muench method. Total RNA was extracted from collected cells and the PRRSV N gene copies and relative expression levels of IFN-α, IFN-β and IFN-γ were quantified using qRT-PCR.

To quantify PRRSV N gene copies by qRT-PCR, a 144 bp fragment of PRRSV N gene was amplified using primers ORF7-F and ORF7-R (Table 1), the purified PCR product was then cloned into pMD18-T vector (Takara, Japan) and the concentration of plasmid DNA was measured using a multi-volume spectrophotometer system (BioTek Epoch-Tak3, USA). PRRSV viral genomic copy numbers were quantified against a standard curve constructed using serial dilutions of plasmid DNA standards. PRRSV N protein expression levels at 36 h post-infection were detected by IFA and Western blot.

Statistical analysis

Data were expressed as mean ± standard deviation (SD). GraphPad prism 5 was used for statistical analysis. Comparisons between groups were considered statistically significant at $p < 0.05$. Apoptosis Index (AI) was calculated by the ratio of Bax/Bcl-2 expression.

Authors' contributions

YM and EMZ conceived and designed the study. YM and LLL executed the majority of the experiments unless otherwise noted. BBZ and XPW constructed the plasmids. BCH and JMG aided in FCAs analysis. CBW, SQX, QZ and YNS participated in PRRSV replication analysis. YM and LLL drafted the manuscript. GPZ, JAH and EMZ revised the manuscript. All authors critically reviewed the manuscript and provided final approval.

Table 2
PRRSV strain SD16 N gene copies and virus titers.

Cell lines	N gene copy numbers (upper panels) and virus titers (lower panels) at different hours postinfection[a]				
	24	36	48	60	72
Marc-145	75,694 ± 2159	76,472 ± 11217	175,405 ± 36467	117,212 ± 16786	114,338 ± 8750
	5.38 ± 0.22	6.21 ± 0.07	5.71 ± 0.14	5.79 ± 0.14	5.25 ± 0.13
Marc-145-GP5	85,390 ± 4035	149,691 ± 31357**	216,009 ± 2746*	210,396 ± 31441**	213,262 ± 31515***
	6.13 ± 0.13**	6.54 ± 0.07*	5.99 ± 0.14	5.91 ± 0.14	5.59 ± 0.07
Marc-145-GP5$^{\Delta 84\text{-}96}$	7788 ± 1732***	14,193 ± 591***	34,852 ± 2234***	18,893 ± 2817***	32,626 ± 2823***
	3.71 ± 0.07***	3.92 ± 0.14***	4.25 ± 0.13***	4.21 ± 0.07***	4.58 ± 0.07***
Marc-145-GP5$^{\Delta 97\text{-}119}$	90,050 ± 6203	241,092 ± 5335**	170,429 ± 32150	136,378 ± 13452	114,576 ± 14707
	5.50 ± 0.13	5.71 ± 0.14*	6.29 ± 0.19 *	5.67 ± 0.19	4.71 ± 0.14
Marc-145-GFP	82,355 ± 18913	137,841 ± 34558*	198,259 ± 13125	85,338 ± 6716	38,386 ± 1914***
	5.21 ± 0.07	5.92 ± 0.07	5.29 ± 0.19	5.08 ± 0.14*	4.92 ± 0.07

Significant differences *versus* Marc-145 time-matched control cells are indicated as follows.

[a] Data represent mean ± SD, $n=3$.

* $p<0.05$.

** $p<0.01$.

*** $p<0.001$.

Acknowledgments

This study was supported by grants from the National Natural Science Foundation of China (No. 31201883), and the Fundamental Research Funds for the Central Universities (2014YB010), awarded to YM, and the National High-Tech R&D Program of China (No. 2011AA10A208) to EMZ

Appendix A. Supporting information

Supplementary data associated with this article can be found in the online version at http://dx.doi.org/10.1016/j.virol.2015.05.019.

References

Amaral, F.R., Bernardes, V.F., Duarte, A.P., Pereira, N.B., Vasconcelos, A.C., Gomez, R. S., Gomes, C.C., 2011. Quantitative expression analysis of apoptotic/antiapoptotic genes and association with immunolocalization of BAX and BCL-2 in peripheral and central giant cell lesions of the jaws. Tumour Biol. 32, 997–1003.

Bautista, E.M., Molitor, T.W., 1999. IFN gamma inhibits porcine reproductive and respiratory syndrome virus replication in macrophages. Arch. Virol. 144, 1191–1200.

Choi, C., Chae, C., 2002. Expression of tumour necrosis factor-alpha is associated with apoptosis in lungs of pigs experimentally infected with porcine reproductive and respiratory syndrome virus. Res. Vet. Sci. 72, 45–49.

Chulu, J.L., Huang, W.R., Wang, L., Shih, W.L., Liu, H.J., 2010. Avian reovirus nonstructural protein p17-induced G(2)/M cell cycle arrest and host cellular protein translation shutoff involve activation of p53-dependent pathways. J. Virol. 84, 7683–7694.

Collins, J.E., Benfield, D.A., Christianson, W.T., Harris, L., Hennings, J.C., Shaw, D.P., Goyal, S.M., McCullough, S., Morrison, R.B., Joo, H.S., et al., 1992. Isolation of swine infertility and respiratory syndrome virus (isolate ATCC VR-2332) in North America and experimental reproduction of the disease in gnotobiotic pigs. J. Vet. Diagn. Investig. 4, 117–126.

Costers, S., Lefebvre, D.J., Delputte, P.L., Nauwynck, H.J., 2008. Porcine reproductive and respiratory syndrome virus modulates apoptosis during replication in alveolar macrophages. Arch. Virol. 153, 1453–1465.

Dea, S., Gagnon, C.A., Mardassi, H., Pirzadeh, B., Rogan, D., 2000. Current knowledge on the structural proteins of porcine reproductive and respiratory syndrome (PRRS) virus: comparison of the North American and European isolates. Arch. Virol. 145, 659–688.

Dokland, T., 2010. The structural biology of PRRSV. Virus Res. 154, 86–97.

Dove, B., Brooks, G., Bicknell, K., Wurm, T., Hiscox, J.A., 2006. Cell cycle perturbations induced by infection with the coronavirus infectious bronchitis virus and their effect on virus replication. J. Virol. 80, 4147–4156.

Fang, Y., Snijder, E.J., 2010. The PRRSV replicase: exploring the multifunctionality of an intriguing set of nonstructural proteins. Virus Res. 154, 61–76.

Feng, L., Zhang, X., Xia, X., Li, Y., He, S., Sun, H., 2013. Generation and characterization of a porcine endometrial endothelial cell line susceptible to porcine reproductive and respiratory syndrome virus. Virus Res. 171, 209–215.

Fernandez, A., Suarez, P., Castro, J.M., Tabares, E., Diaz-Guerra, M., 2002. Characterization of regions in the GP5 protein of porcine reproductive and respiratory syndrome virus required to induce apoptotic cell death. Virus Res. 83, 103–118.

Firth, A.E., Zevenhoven-Dobbe, J.C., Wills, N.M., Go, Y.Y., Balasuriya, U.B., Atkins, J.F., Snijder, E.J., Posthuma, C.C., 2011. Discovery of a small arterivirus gene that overlaps the GP5 coding sequence and is important for virus production. J. Gen. Virol. 92, 1097–1106.

Gagnon, C.A., Lachapelle, G., Langelier, Y., Massie, B., Dea, S., 2003. Adenoviral-expressed GP5 of porcine respiratory and reproductive syndrome virus differs in its cellular maturation from the authentic viral protein but maintains known biological functions. Arch. Virol. 148, 951–972.

Gomez-Laguna, J., Salguero, F.J., Fernandez de Marco, M., Barranco, I., Rodriguez-Gomez, I.M., Quezada, M., Carrasco, L., 2013. Type 2 Porcine reproductive and respiratory syndrome virus infection mediated apoptosis in B- and T-cell areas in lymphoid organs of experimentally infected pigs. Transbound. Emerg. Dis. 60, 273–278.

Hong, H.X., Zhang, Y.M., Xu, H., Su, Z.Y., Sun, P., 2007. Immortalization of swine umbilical vein endothelial cells with human telomerase reverse transcriptase. Mol. Cells 24, 358–363.

Johnson, C.R., Griggs, T.F., Gnanandarajah, J., Murtaugh, M.P., 2011. Novel structural protein in porcine reproductive and respiratory syndrome virus encoded by an alternative ORF5 present in all arteriviruses. J. Gen. Virol. 92, 1107–1116.

Kim, T.S., Benfield, D.A., Rowland, R.R., 2002. Porcine reproductive and respiratory syndrome virus-induced cell death exhibits features consistent with a non-typical form of apoptosis. Virus Res. 85, 133–140.

Lee, C., Rogan, D., Erickson, L., Zhang, J., Yoo, D., 2004. Characterization of the porcine reproductive and respiratory syndrome virus glycoprotein 5 (GP5) in stably expressing cells. Virus Res. 104, 33–38.

Lee, S.M., Kleiboeker, S.B., 2007. Porcine reproductive and respiratory syndrome virus induces apoptosis through a mitochondria-mediated pathway. Virology 365, 419–434.

Li, G., Park, H.U., Liang, D., Zhao, R.Y., 2010. Cell cycle G2/M arrest through an S phase-dependent mechanism by HIV-1 viral protein R. Retrovirology 7, 59.

Liu, C., Liu, C.J., Yuan, X.G., Zhang, C., 2013. Purification and characterization of recombinant envelope protein GP5 of porcine reproductive and respiratory syndrome virus from *E. coli*. J. Chromatogr. A 1304, 133–137.

Luo, R., Fang, L., Jin, H., Jiang, Y., Wang, D., Chen, H., Xiao, S., 2011. Antiviral activity of type I and type III interferons against porcine reproductive and respiratory syndrome virus (PRRSV). Antiviral Res. 91, 99–101.

Ma, Z., Wang, Y., Zhao, H., Xu, A.T., Tang, J., Feng, W.H., 2013. Porcine reproductive and respiratory syndrome virus nonstructural protein 4 induces apoptosis dependent on its 3C-like serine protease activity. PLoS One 8, e69387.

Miller, L.C., Fox, J.M., 2004. Apoptosis and porcine reproductive and respiratory syndrome virus. Vet. Immunol. Immunopathol. 102, 131–142.

Music, N., Gagnon, C.A., 2010. The role of porcine reproductive and respiratory syndrome (PRRS) virus structural and non-structural proteins in virus pathogenesis. Anim. Health Res. Rev. 11, 135–163.

Overend, C., Mitchell, R., He, D., Rompato, G., Grubman, M.J., Garmendia, A.E., 2007. Recombinant swine beta interferon protects swine alveolar macrophages and MARC-145 cells from infection with porcine reproductive and respiratory syndrome virus. J. Gen. Virol. 88, 925–931.

Plagemann, P.G., 2004a. GP5 ectodomain epitope of porcine reproductive and respiratory syndrome virus, strain Lelystad virus. Virus Res. 102, 225–230.

Plagemann, P.G., 2004b. The primary GP5 neutralization epitope of North American isolates of porcine reproductive and respiratory syndrome virus. Vet. Immunol. Immunopathol. 102, 263–275.

Salakou, S., Kardamakis, D., Tsamandas, A.C., Zolota, V., Apostolakis, E., Tzelepi, V., Papathanasopoulos, P., Bonikos, D.S., Papapetropoulos, T., Petsas, T., Dougenis,

D., 2007. Increased Bax/Bcl-2 ratio up-regulates caspase-3 and increases apoptosis in the thymus of patients with myasthenia gravis. In Vivo 21, 123–132.
Sirinarumitr, T., Zhang, Y., Kluge, J.P., Halbur, P.G., Paul, P.S., 1998. A pneumovirulent United States isolate of porcine reproductive and respiratory syndrome virus induces apoptosis in bystander cells both in vitro and in vivo. J. Gen. Virol. 79 (Pt 12), 2989–2995.
Snijder, E.J., Meulenberg, J.J., 1998. The molecular biology of arteriviruses. J. Gen. Virol. 79 (Pt 5), 961–979.
Suarez, P., 2000. Ultrastructural pathogenesis of the PRRS virus. Vet. Res. 31, 47–55.
Suarez, P., Diaz-Guerra, M., Prieto, C., Esteban, M., Castro, J.M., Nieto, A., Ortin, J., 1996. Open reading frame 5 of porcine reproductive and respiratory syndrome virus as a cause of virus-induced apoptosis. J. Virol. 70, 2876–2882.
Sur, J.H., Doster, A.R., Christian, J.S., Galeota, J.A., Wills, R.W., Zimmerman, J.J., Osorio, F.A., 1997. Porcine reproductive and respiratory syndrome virus replicates in testicular germ cells, alters spermatogenesis, and induces germ cell death by apoptosis. J. Virol. 71, 9170–9179.
Sur, J.H., Doster, A.R., Osorio, F.A., 1998. Apoptosis induced in vivo during acute infection by porcine reproductive and respiratory syndrome virus. Vet. Pathol. 35, 506–514.
Thaa, B., Sinhadri, B.C., Tielesch, C., Krause, E., Veit, M., 2013. Signal peptide cleavage from GP5 of PRRSV: a minor fraction of molecules retains the decoy epitope, a presumed molecular cause for viral persistence. PLoS One 8, e65548.
Tian, K., Yu, X., Zhao, T., Feng, Y., Cao, Z., Wang, C., Hu, Y., Chen, X., Hu, D., Tian, X., Liu, D., Zhang, S., Deng, X., Ding, Y., Yang, L., Zhang, Y., Xiao, H., Qiao, M., Wang, B., Hou, L., Wang, X., Yang, X., Kang, L., Sun, M., Jin, P., Wang, S., Kitamura, Y., Yan, J., Gao, G.F., 2007. Emergence of fatal PRRSV variants: unparalleled outbreaks of atypical PRRS in China and molecular dissection of the unique hallmark. PLoS One 2, e526.
Van Breedam, W., Van Gorp, H., Zhang, J.Q., Crocker, P.R., Delputte, P.L., Nauwynck, H.J., 2010. The M/GP(5) glycoprotein complex of porcine reproductive and respiratory syndrome virus binds the sialoadhesin receptor in a sialic acid-dependent manner. PLoS Pathog. 6, e1000730.
Wang, C., Zhao, Q., Liang, C., Dang, L., Ma, Y., Gao, J., Li, Q., Huang, B., Kong, N., Zhang, C., Zhou, E.M., 2012a. Complete genome sequence of a highly pathogenic porcine reproductive and respiratory syndrome virus variant. J. Virol. 86, 8906.
Wang, F.X., Wen, Y.J., Yang, B.C., Liu, Z., Shi, X.C., Leng, X., Song, N., Wu, H., Chen, L.Z., Cheng, S.P., 2012b. Role of non-structural protein 2 in the regulation of the replication of the porcine reproductive and respiratory syndrome virus in MARC-145 cells: effect of gene silencing and over expression. Vet. Microbiol. 161, 58–65.
Wang, X., Wei, R., Li, Q., Liu, H., Huang, B., Gao, J., Mu, Y., Wang, C., Hsu, W.H., Hiscox, J.A., Zhou, E.M., 2013. PK-15cells transfected with porcine CD163 by PiggyBac transposon system are susceptible to porcine reproductive and respiratory syndrome virus. J. Virol. Methods 193, 383–390.
Wei, Z., Lin, T., Sun, L., Li, Y., Wang, X., Gao, F., Liu, R., Chen, C., Tong, G., Yuan, S., 2012. N-linked glycosylation of GP5 of porcine reproductive and respiratory syndrome virus is critically important for virus replication in vivo. J. Virol. 86, 9941–9951.
Wensvoort, G., Terpstra, C., Pol, J.M., ter Laak, E.A., Bloemraad, M., de Kluyver, E.P., Kragten, C., van Buiten, L., den Besten, A., Wagenaar, F., et al., 1991. Mystery swine disease in The Netherlands: the isolation of Lelystad virus. Vet. Q. 13, 121–130.
Wissink, E.H., Kroese, M.V., van Wijk, H.A., Rijsewijk, F.A., Meulenberg, J.J., Rottier, P. J., 2005. Envelope protein requirements for the assembly of infectious virions of porcine reproductive and respiratory syndrome virus. J. Virol. 79, 12495–12506.
Wissink, E.H., van Wijk, H.A., Kroese, M.V., Weiland, E., Meulenberg, J.J., Rottier, P.J., van Rijn, P.A., 2003. The major envelope protein, GP5, of a European porcine reproductive and respiratory syndrome virus contains a neutralization epitope in its N-terminal ectodomain. J. Gen. Virol. 84, 1535–1543.
Wu, W.H., Fang, Y., Farwell, R., Steffen-Bien, M., Rowland, R.R., Christopher-Hennings, J., Nelson, E.A., 2001. A 10-kDa structural protein of porcine reproductive and respiratory syndrome virus encoded by ORF2b. Virology 287, 183–191.
Xu, L.G., Wang, Y.Y., Han, K.J., Li, L.Y., Zhai, Z., Shu, H.B., 2005. VISA is an adapter protein required for virus-triggered IFN-beta signaling. Mol. Cell 19, 727–740.
Xu, X., Zhang, H., Zhang, Q., Huang, Y., Dong, J., Liang, Y., Liu, H.J., Tong, D., 2013. Porcine epidemic diarrhea virus N protein prolongs S-phase cell cycle, induces endoplasmic reticulum stress, and up-regulates interleukin-8 expression. Vet. Microbiol. 164, 212–221.
Yang, Q., Gao, L., Si, J., Sun, Y., Liu, J., Cao, L., Feng, W.H., 2013. Inhibition of porcine reproductive and respiratory syndrome virus replication by flavaspidic acid AB. Antiviral Res. 97, 66–73.
Zaulet, M., Gurau, M.R., Petrovan, V., Buburuzan, L., 2012. Genetic diversity characterization of porcine reproductive and respiratory syndrome virus isolates in romania, based on phylogenetic analysis. Int. J. Mol. Sci. 13, 12046–12061.
Zhao, R.Y., Elder, R.T., 2005. Viral infections and cell cycle G2/M regulation. Cell Res. 15, 143–149.